Supporting Information

A scalable slurry process to 3D lithiophilic and conductive framework for high performance lithium metal anode

Yuanming Liu,[a,b] [1] Xianying Qin,[a,d] [1] Shaoqiong Zhang,[a,b] Lihan Zhang,[a,b] Feiyu Kang,[a,b,c] Guohua Chen,[d,]* Xiangfeng Duan,[e,]* Baohua Li[a,c]*

[a] Engineering Laboratory for Next Generation Power and Energy Storage Batteries, Engineering Laboratory for Functionalized Carbon Materials, Graduate School at Shenzhen, Tsinghua University, Shenzhen 518055, China.
[b] School of Materials Science and Engineering, Tsinghua University, Beijing 100084,China.
[c] Shenzhen Geim Graphene Center, Shenzhen 518055, China.
[d] Department of Mechanical Engineering, The Hong Kong Polytechnic University, Hong Kong, China.
[e] Department of Chemistry and Biochemistry, University of California, Los Angeles, CA 90095, USA.

[1] These authors contributed equally to this work.
*Corresponding authors:
guohua.chen@polyu.edu.hk (G. Chen)
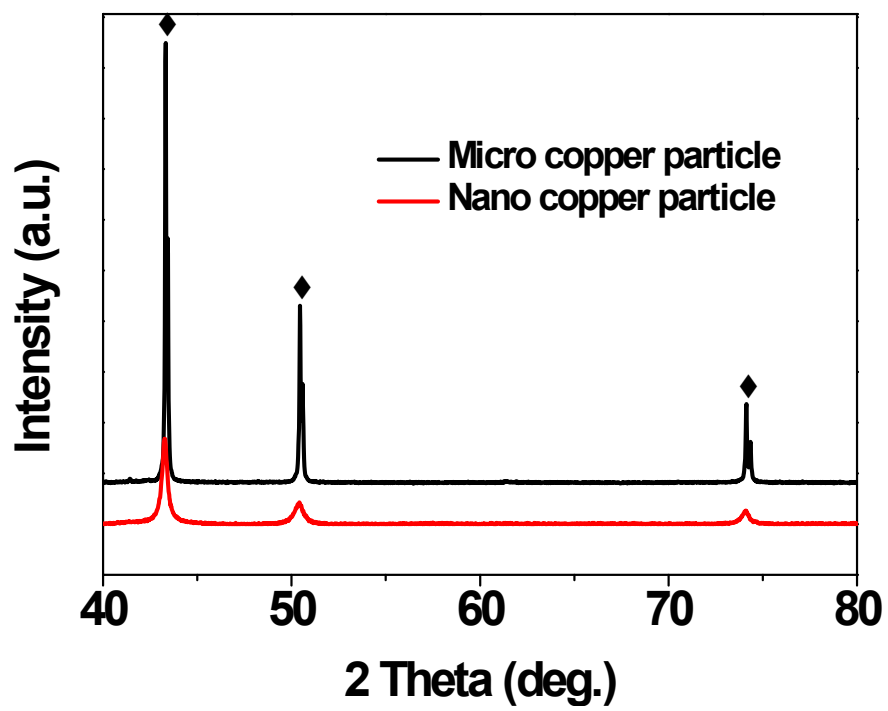xduan@chem.ucla.edu (X. Duan)
libh@mail.sz.tsinghua.edu.cn (B. Li)

Figure S1. XRD patterns of Cu micro- and nano-particles.
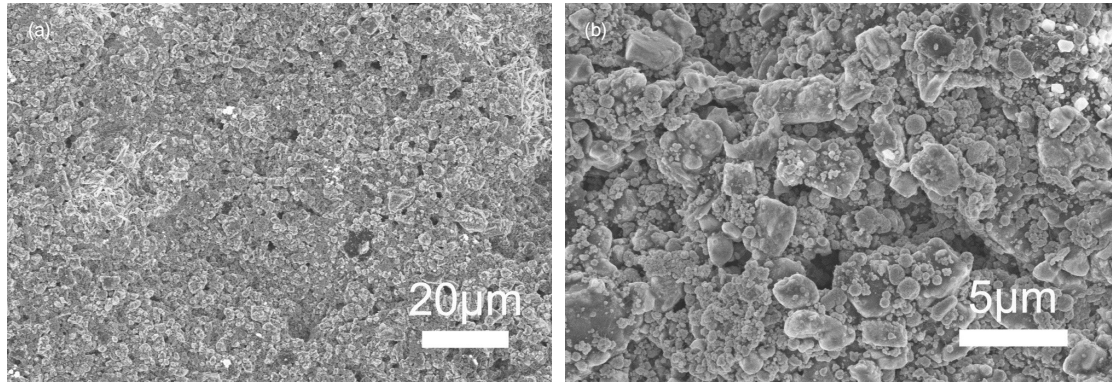
Figure S2. (a), (b) Front SEM images of CCP-mix current collector after slurry coating and drying process under different magnifications.
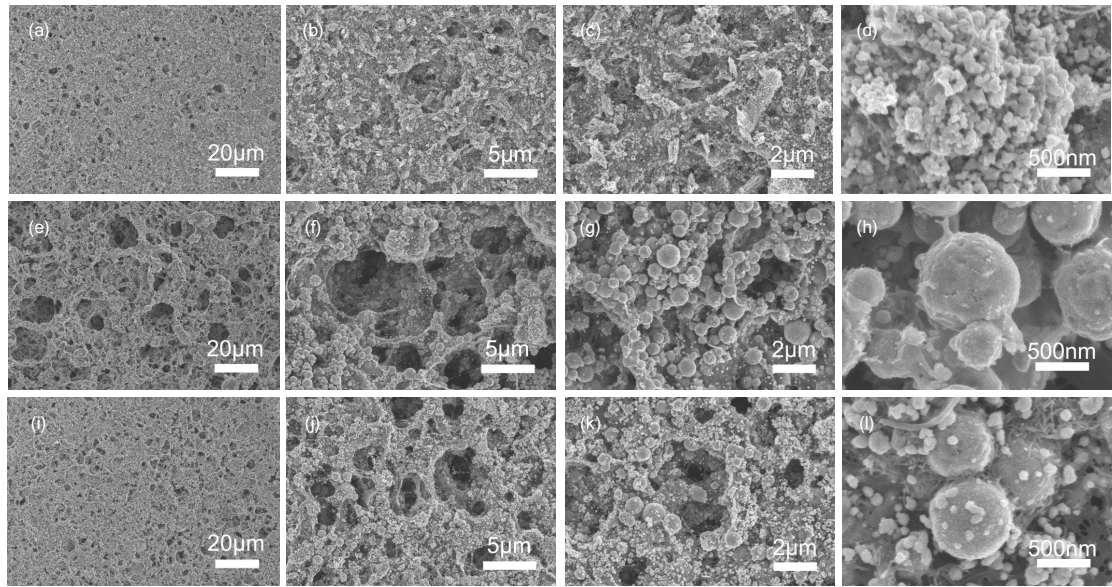
Figure S3. SEM images of top surface of various 3D porous hybrid Cu current collectors under different magnifications: (a, b, c, d) CCP-nano; (e, f, g, h) CCP-micro; (i, j, k, l) CCP-mix.
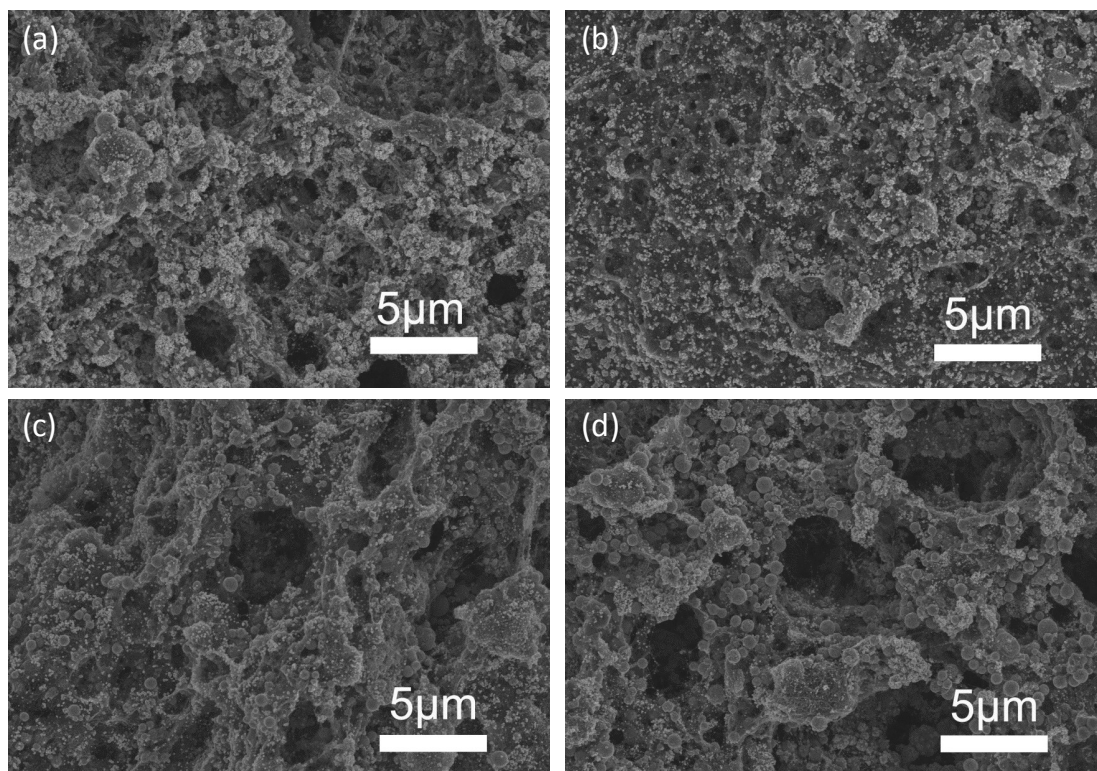
Figure S4. SEM images of CCP-mix electrodes with different ratio of micro- and nano- copper particles: (a) 1:1; (b) 2:1; (c) 3:1; (d) 4:1.
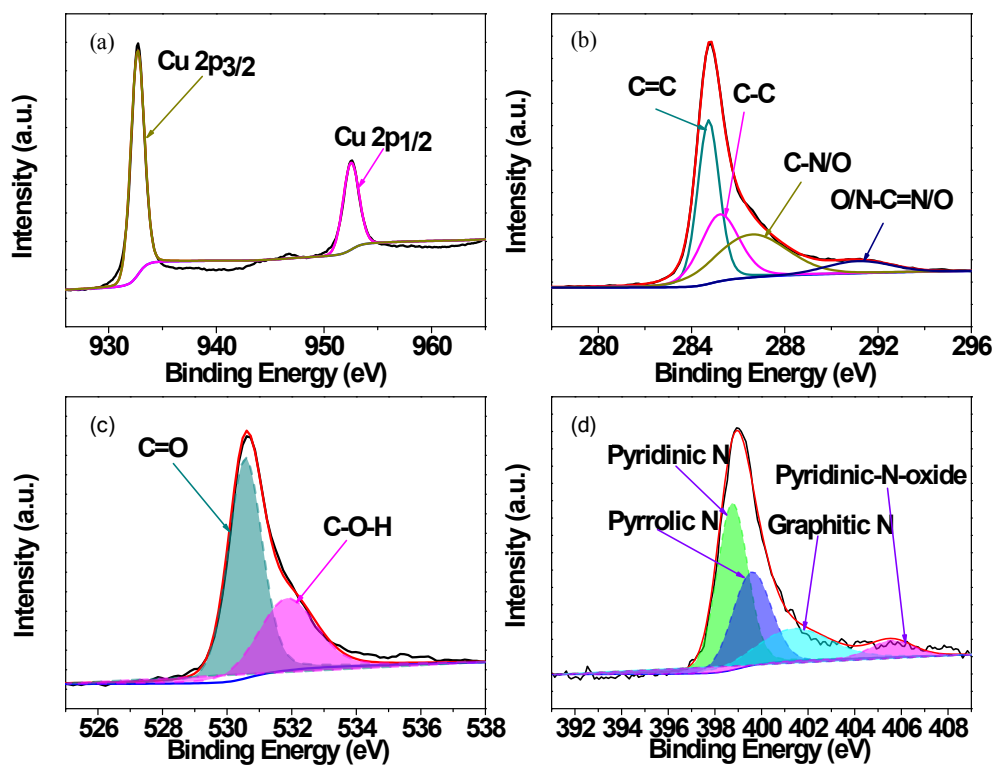
Figure S5. XPS spectrum of (a) Cu 2p; (b) C1s; (c) O1s and (d) N1s of CCP-mix current collector.

Table S1. Mass percent of each elements of CCP-mix current collector and each categories of oxygen and nitrogen atoms through XPS analysis.

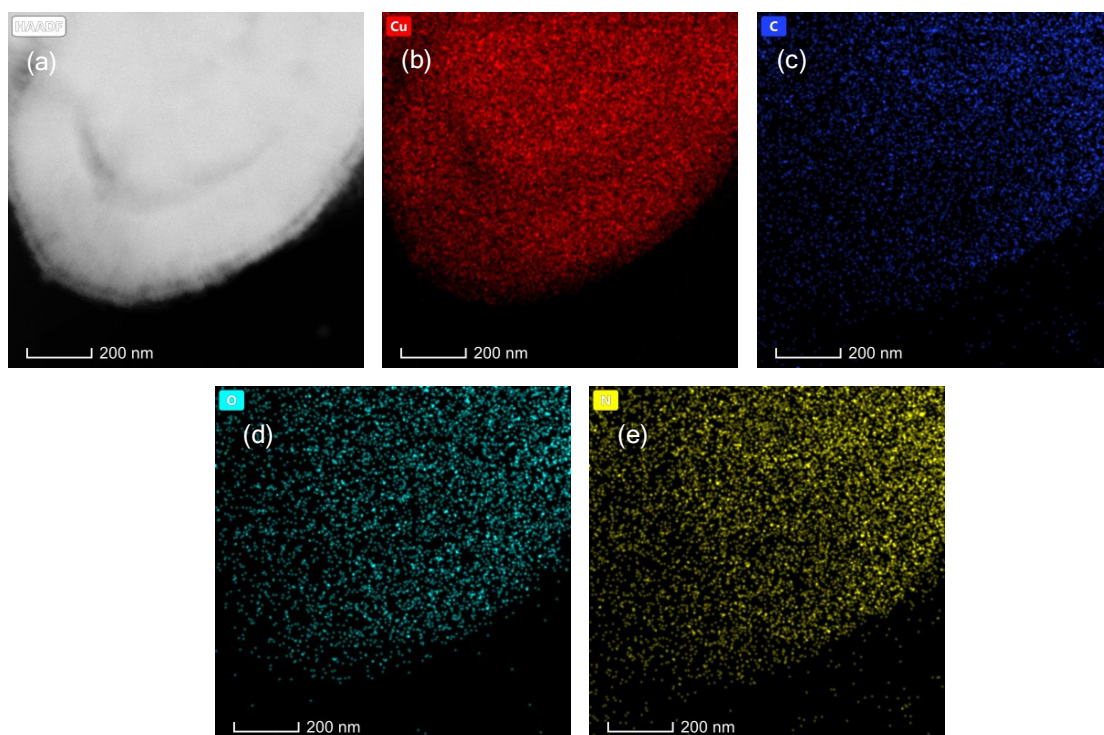| Element	Cu	C	N	O
Mass percent(%)	42.5	40.82	5.08	11.6
Category of oxygen atom	Carbonyl	Alkoxy		
Mass percent(%)	64.52	35.48		
Category of nitrogen atom	Pyridinic N	Pyrrolic N	Graphitic N	Pyridinic-N-oxide
Mass percent(%)	43.88	29.28	20.78	6.06

Figure S6. (a) STEM image of CCP-mix coating layer; (b, c, d, e) Corresponding EDX mapping results of element Cu, C, O, N.
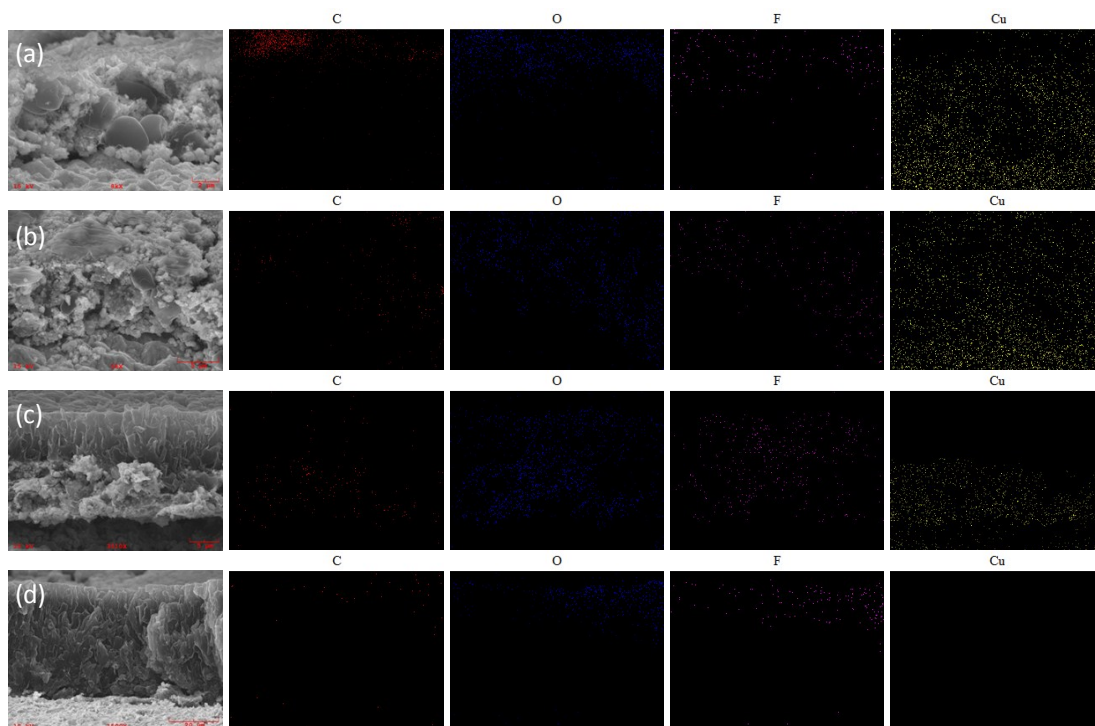
Figure S7. Elemental mapping results for the CCP-mix @ Li electrodes with (a) 0.5 mAh cm^{-2}; (b) 1 mAh cm^{-2}; (c) 2 mAh cm^{-2} and (d) 6 mAh cm^{-2} of Li deposition.

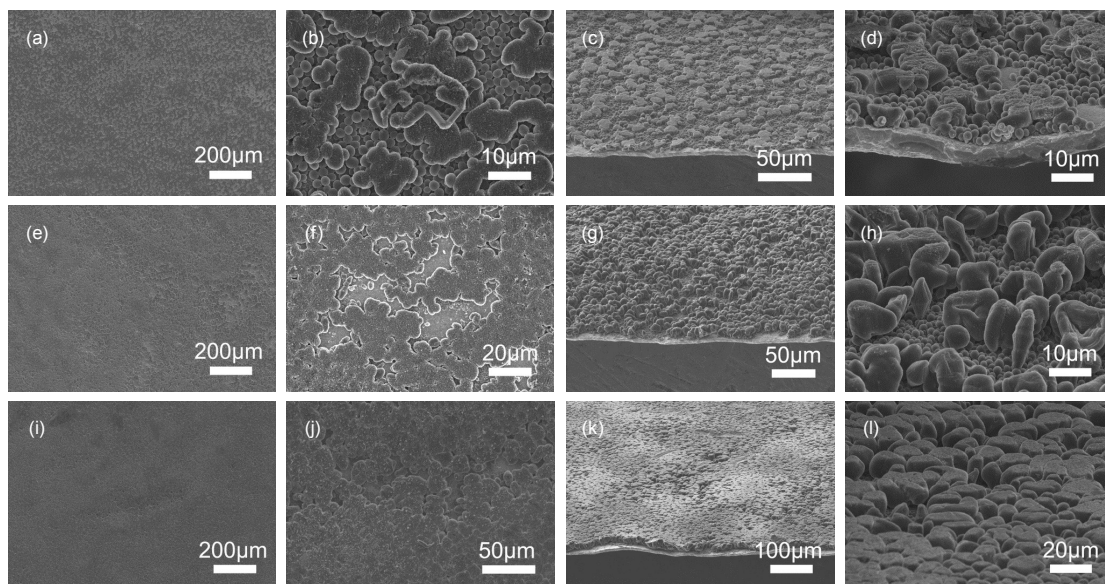**Figure S8.** SEM images of Li deposited on Planar Cu foil at 1 mA cm^{-2} with various Li capacities: (a, b, c, d) 1 mAh cm^{-2}, (e, f, g, h) 2 mAh cm^{-2}, (i, j, k, l) 6 mAh cm^{-2}.
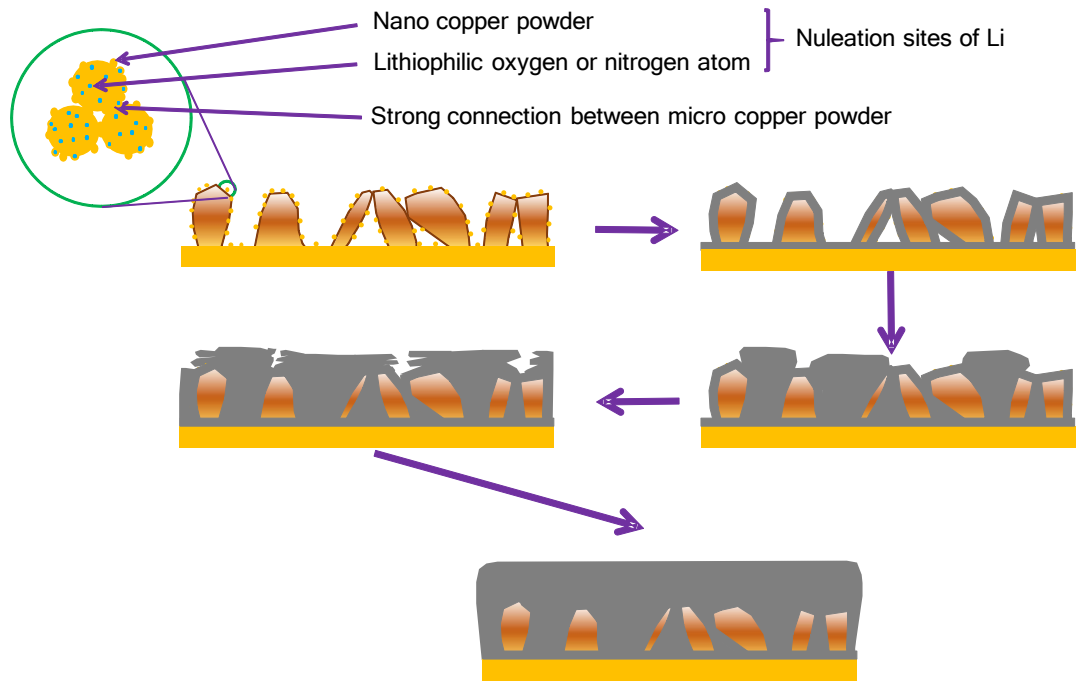
Figure S9. Schematic diagrams of the nucleation and growth processes of Li on CCP-mix current collector.
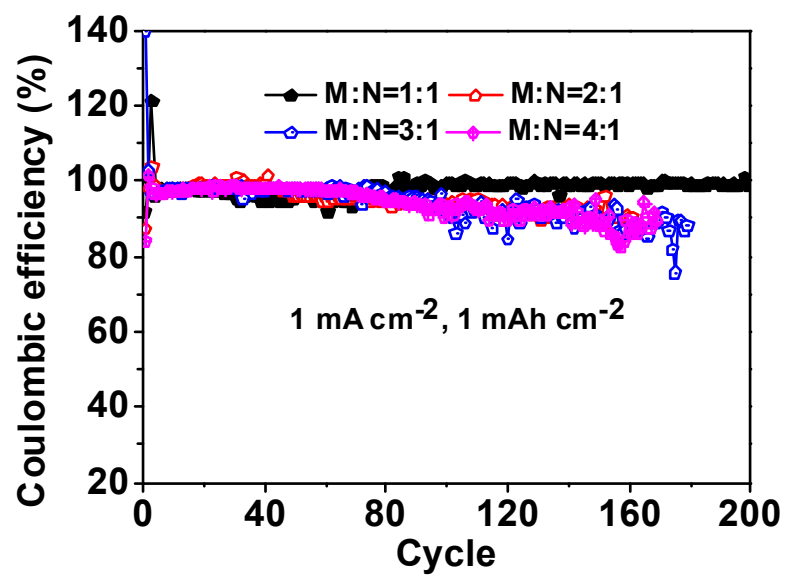
Figure S10. Coulombic efficiency of CCP-mix electrodes with different mass ratio of micro- and nano-copper particles.
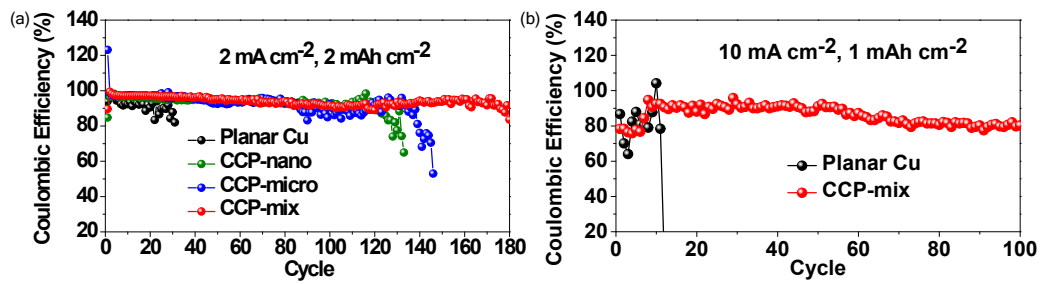
Figure S11. Coulombic efficiencies of Planar Cu, CCP-nano, CCP-micro and CCP-mix current collector with deposition capacity and current density of: (a) 2 mAh cm^{-2} and 2 mA cm^{-2}; (b) 1 mAh cm^{-2} and 10 mA cm^{-2}.

Table S2. Comparison of Coulombic efficiencies of 3D hybrid Cu network current collector (CCP-mix) to other state of art modifications.

Scaffold	Current density (mA cm^{-2})	Capacity (mAh cm^{-2})	Coulombic Efficiency (%)	Cycles	Electrolyte	Reference
N-doped graphitic carbon	2	2	99.6	300	1M LiTFSI DOL/DME, 2% LiNO$_3$	Adv. Mater., 2018, 30, 1706216.
	2	6	99.4	150		
	2	8	99.1	140		
Crumpled graphene balls	0.5	0.5	97.5	700	1M LiTFSI DOL/DME, 1% LiNO$_3$	Joule, 2018, 2, 184-193
	1	1	97.5	120		
	3	1	96	170		
	1	2	95	190		
	1	12	96	40		
Double layer diamond interfaces	0.5	0.5	99	200	1M LiTFSI DOL/DME	Joule,2018, 2, 1595-1609
	0.5	1	99	150		
	1	1	99	150		
	1	2	98.4	150		
Engineering stable interfaces	0.5	1	99	500	1M LiTFSI DOL/DME, 5% LiNO$_3$	Sci. Adv. 2018, 4, eaat5168
LiNO$_3$ protected glass fiber	1	1	92.2	242	1M LiPF$_6$ EC/DEC	PNAS, 2018, 115, 5676-5680
	4	1	93.7	240		
	1	5	98.3	160		
	5	10	98.1	53		
Cu-CuO-Ni hybrid structure	1	1	95	250	1M LiTFSI DOL/DME, 1% LiNO$_3$	Adv. Mater. 2018, 29, 1705830
	3	0.5	95	90		

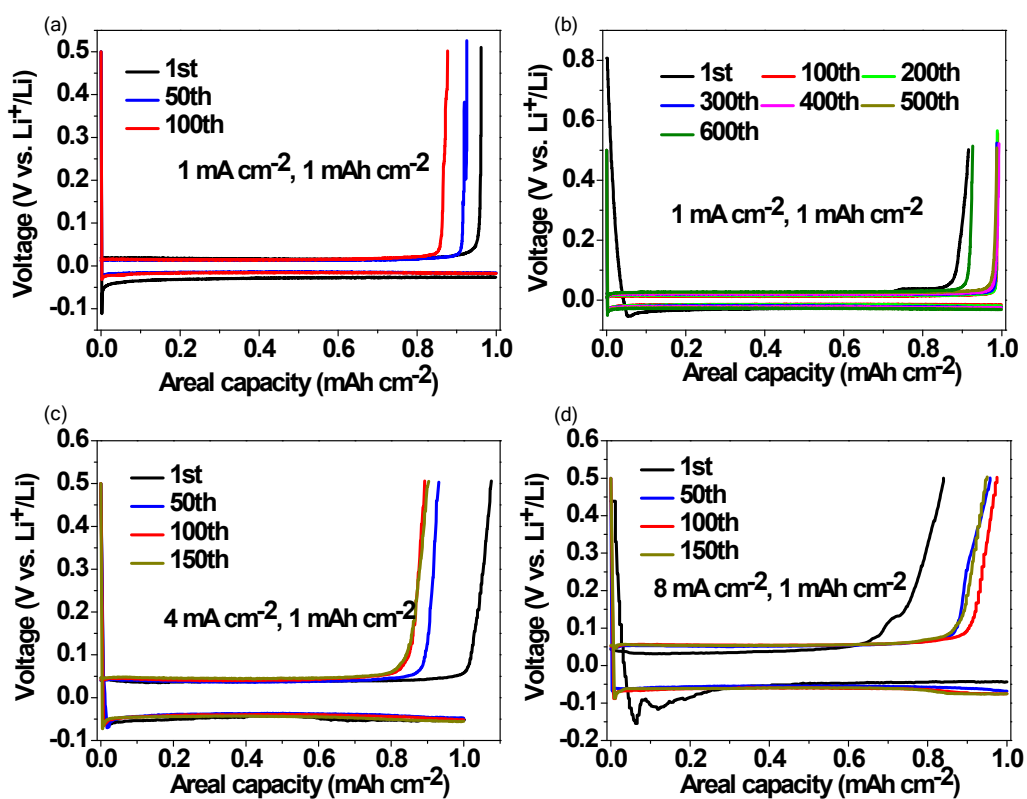| Material					Electrolyte	Reference
N-doped graphene decorated Cu foam	0.5	1	97	150	1M LiTFSI DOL/DME, 1% LiNO$_3$	Adv. Funct. Mater., 2018, 27, 1606422
	0.5	4	97	100		
	1	2	97	50		
3D PMF coating	1	1	95.8	300	1M LiTFSI DOL/DME, 2% LiNO$_3$	Adv. Energy. Mater., 2018, 1703360
	1	3	97.5	120		
	3	1	97.4	140		
	5	1	95.6	100		
	10	1	94.7	50		
3 D hybrid Cu network (CCP-mix)	**1**	**1**	**98.8**	**500**	**1M LiTFSI DOL/DME, 1% LiNO$_3$**	**This work**
	1	**4**	**91.6**	**100**		
	4	**1**	**92**	**169**		
	8	**1**	**92.22**	**160**		
	10	**1**	**80.3**	**100**		
	12	**1**	**91**	**70**		

Figure S12. The voltage-capacity profiles of (a) Li/planar Cu cell at 1 mA cm^{-2} with Li capacity of 1 mAh cm^{-2} at specific cycles and (b,c,d) Li/CCP-mix cells at (b) 1 mA cm^{-2}, (c) 4 mA cm^{-2}, (d) 8 mA cm^{-2} with Li capacity of 1 mAh cm^{-2} at specific cycles.
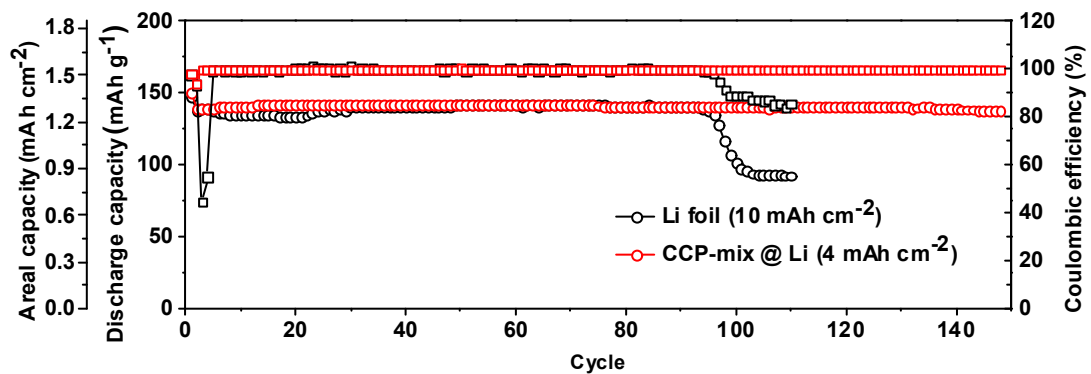
Figure S13. Electrochemical performance of Li | LFP full cell with low N/P ratio of 2.16 (CCP-mix electrode) and 5.41 (Li foil).
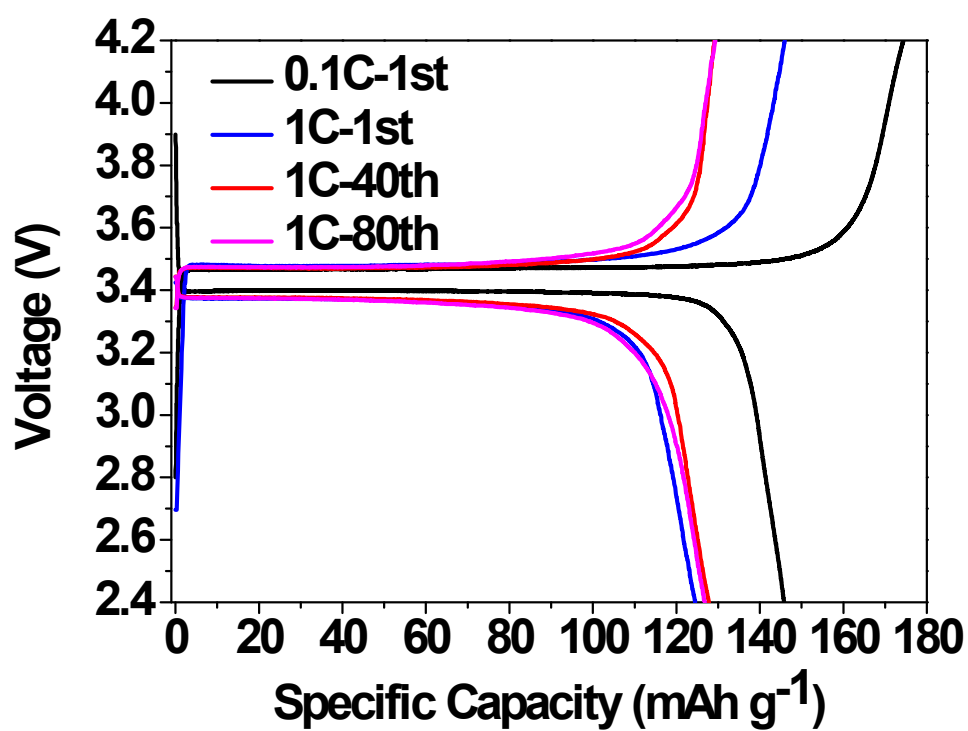
Figure S14. Corresponding voltage-capacity profiles of full cells with CCP-mix@Li anode and LiFePO$_4$ cathode at 0.1 C and 1 C for specific cycles.
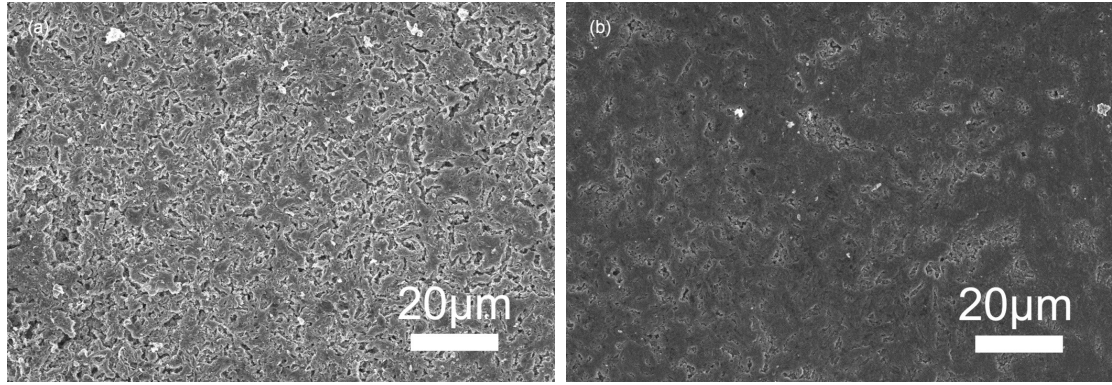
Figure S15. SEM images of (a) planar Cu and (b) CCP-mix samples after repeated Li plating and stripping for 100 cycles at 1 mA cm^{-2} with Li capacity of 1 mAh cm^{-2}.
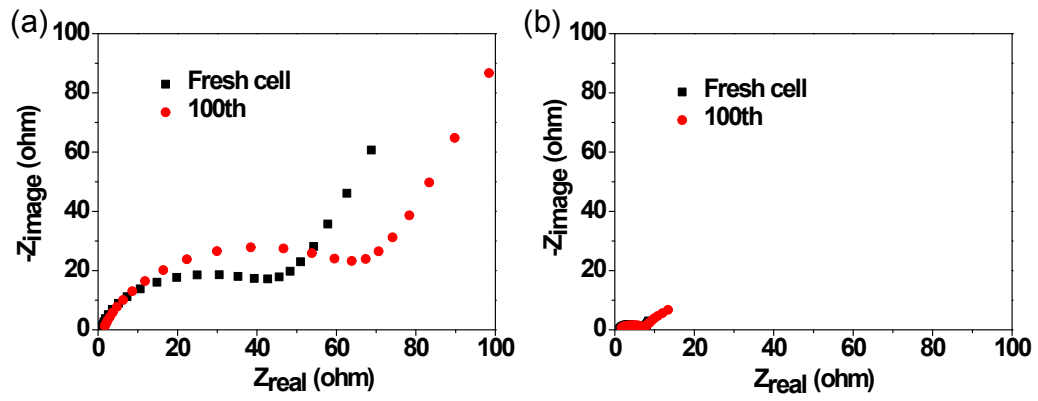
Figure S16. The Nyquist curves of fresh cells and cycled cells after repeated plating and stripping Li at 1 mA cm^{-2} with Li capacity of 1 mAh cm^{-2} for 100 cycles of (a) Planar Cu and (b) CCP-mix samples.

S1: Explanation of the nanosized Cu particles to act as the sintering additive of Cu microparticles.

As the literature reported[1], for the melting point T_m of nanosized Cu particles:

$$T_m = T_0 \exp\left(-\frac{2\sigma M}{\rho_m \Delta_{fus} H_m \frac{1}{r}}\right)$$

where T_0 is the melting point of the normal bulk materials; M is the molar mass of metal Cu; σ is the specific surface free energy; ρ_m is the density; $\Delta_{fus} H_m$ is the molar enthalpy of fusion and r is the diameter of nanosized Cu particles.

Because of the smaller diameter (r) of nanosized Cu particles, it shows the higher specific surface free energy, thus delivers higher chemical potential than bulk materials, inducing the lower melting point and sintering temperature of it. Moreover, smaller the particle diameter is, the lower the melting point and sintering temperature will be.

For the Cu based materials, Liu el al.[2] has reported that the nanosized Cu particles with average diameter of 40 to 50 nm would melt at 477 °C. When the ramp rate is lower than 30 °C/min, the nanosized Cu particles have enough time to grow bigger, thus show unconspicuous melting point depression. In our case, all we want to do is just construct a stubborn skeleton to withstand the volume expansion caused by repeated plating/stripping of Li and facilitate the ion transfer at the same time. Thus we don't need the fusion of Cu nanoparticles, the higher diffusion of the Cu atom between the micro- and nano- particles is desired in achieving our goals. From the above, 400 °C is the ideal holding temperature for the heat treatment of the CCP-mix electrode.

Notes and references

1.   J. Qu, M. Hu, J. Chen and W. Han, *Earth Science-Journal of China University of Geosciences*, 2005, 195-198.
2.   W. Liu, X. Deng and Z. Zhang, *Physical Testing and Chemical Analysis Part A: Physical Testing*, 2004, 64-67.